

Linkage Transformations in a Three-Dimensional Covalent Organic Framework for High-Capacity Adsorption of Perfluoroalkyl Substances

Andrea N. Zeppuhar, Devin S. Rollins, Dale L. Huber, Emmanuel A. Bazan-Bergamino, Fu Chen, Hayden A. Evans, and Mercedes K. Taylor*



Cite This: *ACS Appl. Mater. Interfaces* 2023, 15, 52622–52630



Read Online

ACCESS |



Metrics & More



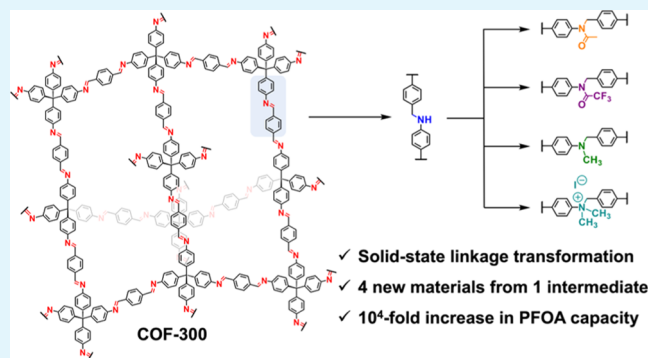
Article Recommendations



Supporting Information

ABSTRACT: Despite their many advantages, covalent organic frameworks (COFs) built from three-dimensional monomers are synthetically difficult to functionalize. Herein, we provide a new synthetic approach to the functionalization of a three-dimensional covalent organic framework (COF-300) by using a series of solid-state linkage transformations. By reducing the imine linkages of the framework to amine linkages, we produced a more hydrolytically stable material and liberated a nucleophilic amino group, poised for further functionalization. We then treated the amine-linked COF with diverse electrophiles to generate a library of functionalized materials, which we tested for their ability to adsorb perfluoroalkyl substances (PFAS) from water. The framework functionalized with dimethylammonium groups, COF-300-dimethyl, adsorbed more than 250 mg of perfluorooctanoic acid (PFOA) per 1 g of COF, which represents an approximately 14,500-fold improvement over that of COF-300 and underscores the importance of electrostatic interactions to PFAS adsorption performance. This work provides a conceptually new approach to the design and synthesis of functional three-dimensional COFs.

KEYWORDS: adsorption, covalent organic frameworks, perfluoroalkyl substances, porous materials, solid-state reactions



INTRODUCTION

The porosity, crystallinity, and relative stability of covalent organic frameworks (COFs) make them promising adsorbents for the removal of contaminants from water. These organic networks can effectively separate metal ions,^{1–3} organic dyes,^{4,5} and perfluoroalkyl substances (PFAS)^{6–8} from aqueous solution. However, designing a COF for a particular separation tends to require the laborious synthesis of custom monomers, which must then be incorporated into frameworks, which are then tested as adsorbents. The need to functionalize monomers in the early stages of COF synthesis prevents chemists from rapidly establishing structure–property relationships and leads to costly and time-intensive synthetic routes. Alternatively, it has been shown that COFs can undergo chemical transformations, postsynthetically, to add additional functionality without altering the existing framework.^{9–17} This strategy is particularly useful for three-dimensionally linked (3D) COFs, whose monomers draw from a limited selection of tetrahedral building blocks. We sought to expand the range of functionality in 3D COFs because these 3D networks show improved stability and crystallinity compared with their 2D counterparts. With this objective, we hypothesized that if the linkage between monomers was transformed into a nucleophilic

group after COF synthesis, this nucleophilic site would allow us to append a range of diverse functional groups.

We focused our efforts on functional groups that would enhance the adsorption of PFAS from water. Widely used in surfactants, coatings, and fire-fighting foams, this class of micropollutants has spread throughout the global water supply.^{18,19} The strong carbon–fluorine bonds in PFAS prevent their environmental degradation, causing them to be termed “forever chemicals”.^{20,21} Because chronic PFAS exposure is harmful to human health,^{22,23} the removal of PFAS from water has become an urgent area of research.

Researchers have shown that adsorbents with cationic groups^{24–27} or fluorocarbon chains^{8,28,29} interact strongly with the respective components of PFAS adsorbates (Figure 1a). This strategy has borne fruit in the design of PFAS-selective COFs. However, such a COF design typically relies

Received: August 28, 2023

Revised: October 18, 2023

Accepted: October 24, 2023

Published: November 3, 2023



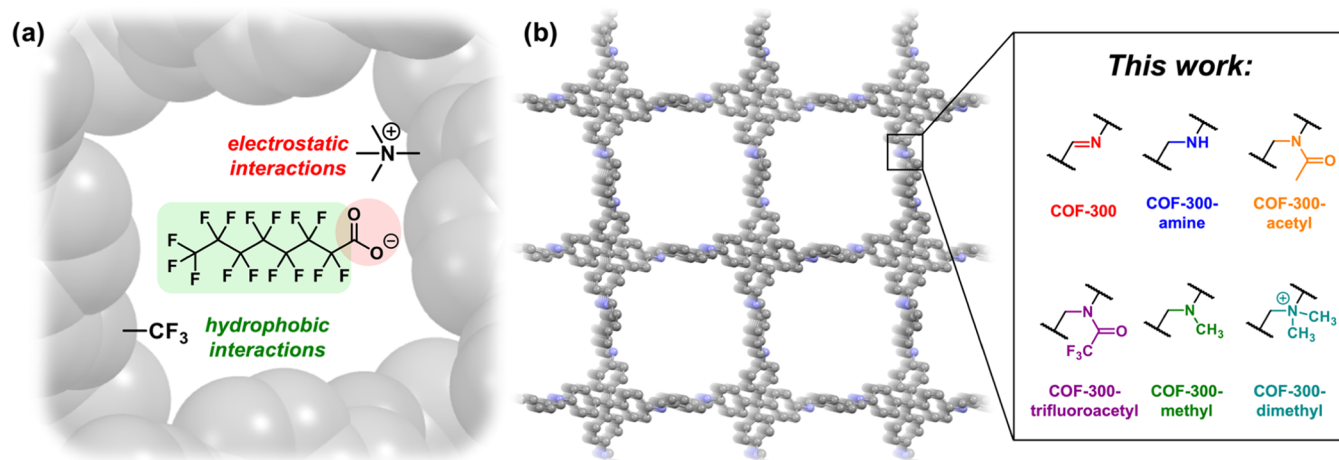


Figure 1. (a) Types of interactions that enhance perfluoroalkyl substance (PFAS) adsorption in porous materials. (b) Modification of covalent organic framework linkages presented in this work. Figure adapted from the COF-300 crystallographic data reported in ref 32.

on the synthesis of bespoke monomers. Rather than painstakingly functionalize a series of monomers at the beginning of a multistep synthetic route, we aimed to functionalize the linkages between monomers in the last step of our COF synthesis.

Linkage functionalization can simultaneously accomplish two crucial tasks: First, reversible linkages can be transformed into more stable bonds that are less prone to hydrolysis, and second, the newly introduced functional groups can improve the adsorption capacity. In this work, we converted the imine linkages of a well-studied three-dimensional framework, COF-300,^{30–34} into secondary, tertiary, or quaternary amines, and we appended acetyl or trifluoroacetyl groups to these linkages (Figure 1b). This synthetic approach led to improved PFAS adsorbents, including a material with outstanding PFAS adsorption capacity (denoted as COF-300-dimethyl; see Figure 1b). Further, this approach provides a general synthetic route to late-stage diversification in imine-linked frameworks, opening a shortcut to a broad library of functionalized 3D COFs.

RESULTS AND DISCUSSION

Synthesis and Characterization. COF-300 was synthesized in a solvothermal method³⁰ by combining 1 equiv (eq) tetrakis(4-aminophenyl)methane (TAPM) with 2 equiv terephthalaldehyde in 1,4-dioxane in the presence of aqueous acetic acid (Scheme 1). Heating the mixture to 120 °C in a sealed vessel for 3 days afforded crystalline COF-300, the formation of which was verified by powder X-ray diffraction (PXRD; Figure S9).

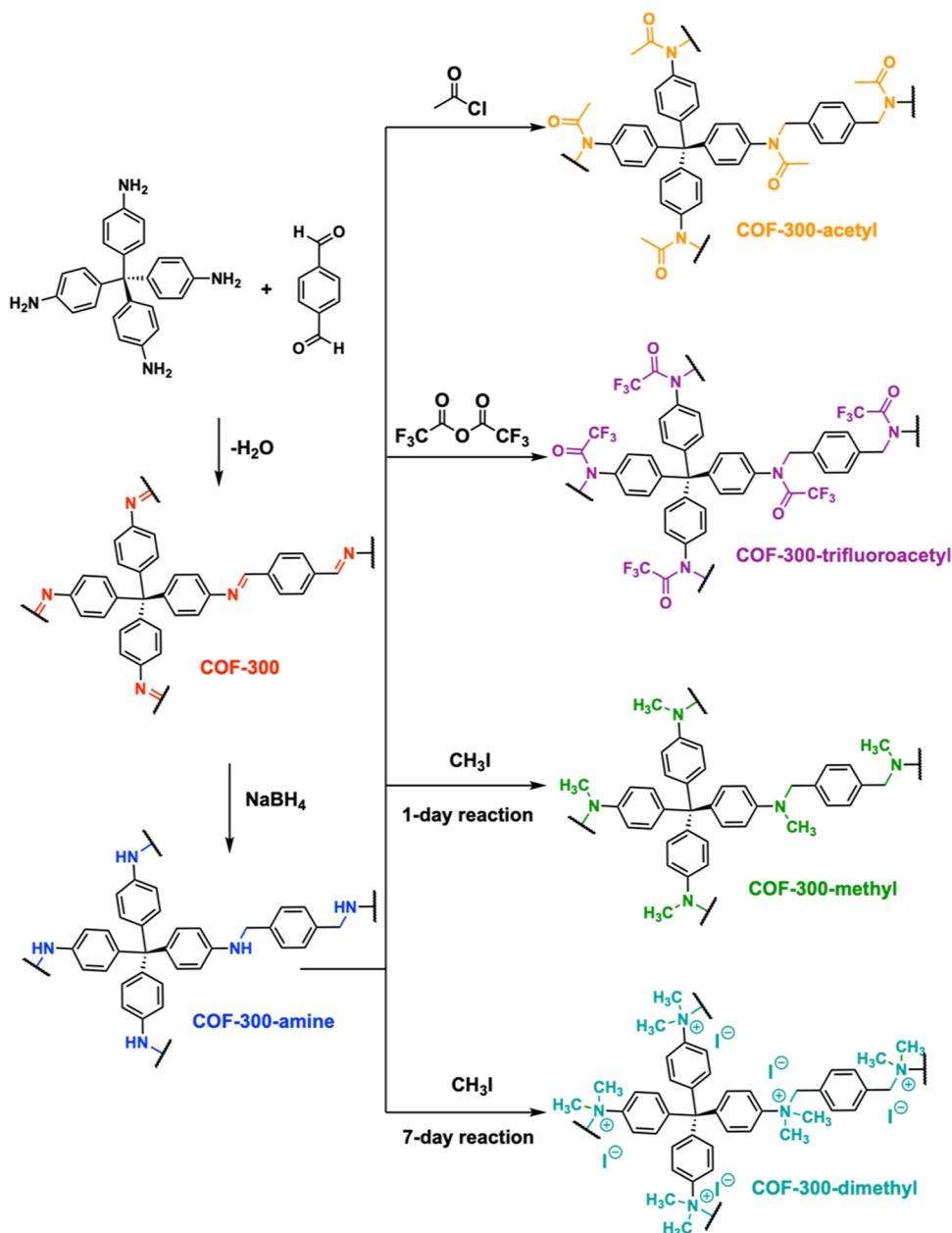
Using a previously reported method,⁹ COF-300 was reduced by treatment with 38 equiv sodium borohydride at room temperature for 24 h to yield the amine-linked structure referred to herein as COF-300-amine (Scheme 1). Complete reduction of COF-300 was verified by using ¹³C solid-state NMR spectroscopy (ssNMR), as shown in Figure 2a (top). Upon reduction, the signal at 155 ppm (corresponding to the imine carbon) disappeared and was replaced by a new signal at 48 ppm, consistent with the formation of an amine linkage. Infrared (IR) spectroscopy provided further confirmation of complete reduction (Figure 2a, bottom): The signal corresponding to the C=N stretch of the imine at 1613

cm⁻¹ disappeared, and new signals at 1606 and 1249 cm⁻¹ indicated amine formation.

After the successful reduction of COF-300, reactions were carried out to functionalize the material. Because amines are readily acylated, COF-300-amine was treated with 10 equiv of acetyl chloride at room temperature for 24 h to produce COF-300-acetyl (Scheme 1). Analysis via ¹³C ssNMR revealed new signals at 167, 53, and 19 ppm, which correspond to the carbonyl carbon, the benzylic carbon, and the methyl carbon, respectively, of the newly formed amide (Figure 2b, top). In addition, IR spectroscopy revealed a new signal at 1658 cm⁻¹, indicating a newly formed carbonyl (Figure 2b, bottom). Based on the absence of the signal at 48 ppm in the ssNMR spectrum, we conclude that the COF-300-amine undergoes complete conversion to the amide product.

Having shown that the COF-300-amine can be readily functionalized, we expanded the reaction scope to groups we expected to enhance PFAS adsorption. To introduce fluorine–fluorine interactions, COF-300-amine was treated with 10 eq. trifluoroacetic anhydride at room temperature for 24 h to produce COF-300-trifluoroacetyl (Scheme 1), and the isolated material was analyzed using ¹³C ssNMR, as shown in Figure 2c (top). The spectrum of the product contains a new signal at 154 ppm, consistent with the carbonyl carbon of the newly formed amide. IR spectroscopy (Figure 2c, bottom) also revealed the presence of a new carbonyl signal at 1701 cm⁻¹, further supporting the amide formation. However, unlike the acetylation described above, the trifluoroacetylation did not appear to go to completion. To better analyze the ssNMR spectrum of COF-300-trifluoroacetyl, we compared it to the solution-state ¹³C NMR spectrum of a molecular analogue (see the SI for details). This analysis showed the ssNMR peak at 54 ppm to represent the benzylic carbon of trifluoroacetylated sites and the peak at 49 ppm to represent the benzylic carbon of unreacted amine sites. By comparing the integration values for these two peaks, we determined that approximately 50% of the amine linkages in COF-300-amine were converted to trifluoroacetyl groups; thus, the material termed COF-300-trifluoroacetyl contains approximately 50% trifluoroacetyl linkages and 50% amine linkages. This incomplete conversion may result from the lower electrophilicity of anhydrides compared to acid chlorides as well as from the steric bulk of the anhydride. Regardless, water contact angle experiments

Scheme 1. Synthesis, Reduction, and Late-Stage Diversification of COF-300



showed that the hydrophobicity of COF-300-trifluoroacetyl was significantly increased compared to that of COF-300-amine, which is a relevant property for PFAS adsorption. A water contact angle of 123° was measured for COF-300-trifluoroacetyl, indicating a hydrophobic material, whereas a water contact angle of only 50° was measured for COF-300-amine (Figures S46–S47).

Because it has been demonstrated that quaternary ammonium groups serve as good binding sites for anionic PFAS molecules,^{24–27} and because secondary amines can be readily dialkylated, our next approach to enhance PFAS adsorption was to react COF-300-amine with 50 eq. methyl iodide in order to produce quaternary ammonium groups throughout the framework (Scheme 1). After 1 day of reaction at room temperature, the isolated material was analyzed via ¹³C ssNMR, as shown in Figure 2d (top). The new, broad signal at 36 ppm is consistent with the methyl carbon of a

monomethylated material, termed COF-300-methyl, based upon comparison to the solution-state ¹³C NMR of the molecular analogue (Figure S4). Doubling the reaction time from 1 day to 2 days led to minimal changes in the outcome. However, extending the reaction time to 7 days substantially increased the dimethylation of the material, yielding a material termed COF-300-dimethyl. The new signal at 71 ppm in the ssNMR spectrum of COF-300-dimethyl is attributed to the benzylic carbon of the dimethylated material, based upon comparison to the solution-state ¹³C NMR of the dimethylated molecular analogue (Figure S4). The ssNMR spectrum for COF-300-dimethyl indicates that only ~40% dimethylation was achieved after 7 days of reaction time, although we note that peak integrations from ssNMR data can yield only approximate values. This percent functionalization is estimated based on the relative integrations of the signals at 36 and 71 ppm, corresponding to monomethylated and dimethylated

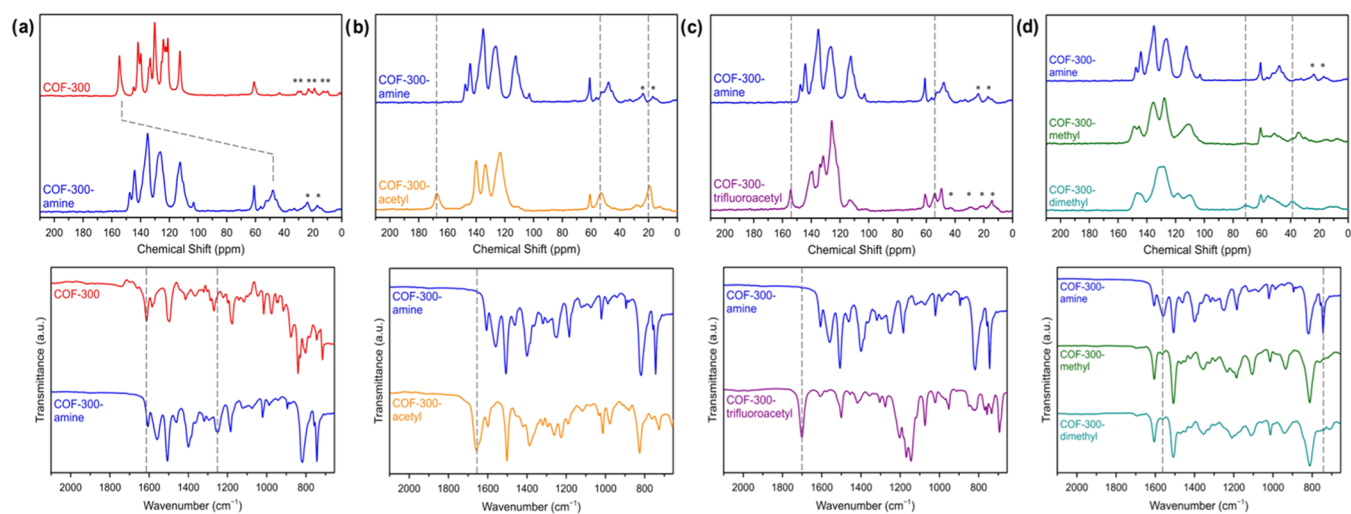


Figure 2. Top row: ¹³C solid-state NMR (ssNMR) spectra; bottom row: infrared (IR) spectra of postsynthetic modification reactions. (a) Reduction of COF-300. (b) Acetylation of COF-300-amine. (c) Trifluoroacetylation of COF-300-amine. (d) Methylation of COF-300-amine. Asterisks (*) denote spinning side bands in the ssNMR spectra.

sites, respectively. Molecular analogue studies also showed the dimethylation reaction to be slow compared to the acylation reactions (see pages S9–S10 for experimental conditions).

The incomplete functionalization observed for COF-300-trifluoroacetyl and COF-300-dimethyl represents a drawback of the linkage transformation strategy described in this work. The postsynthetic modification of porous materials is often hindered by steric constraints of the pore environment and slow diffusion of reagents to the particle interior. While this disadvantage can sometimes be overcome with longer reaction times or greater stoichiometric excesses, it often limits the percent functionalization of a material and prevents precise structural characterization. However, we propose that postsynthetic linkage transformation can confer major synthetic advantages, as a common intermediate can yield a library of functionalized products in the final step of synthesis. Further, even partial functionalization can lead to major improvements in properties such as PFAS adsorption capacity, as discussed below.

In addition to other probes, PXRD was used to determine whether the underlying crystalline framework of COF-300 was retained during the linkage modification reactions. The known crystal structures of COF-300 (activated and hydrated) are reported in space group $I4_1/a$ (space group 88).³² Through Pawley fitting, we found there to be a fundamental difference between the as-synthesized structures of COF-300 and the COF-300-amine (Figure S10). We hypothesize that the conversion of rigid imine bonds to more freely rotating amine bonds introduces new degrees of flexibility into COF-300-amine, thus allowing structural distortion (COF-300 itself has a flexible structure that is dependent on guests in the pores³⁴). To test this hypothesis, PXRD patterns were collected for both COF-300 and COF-300-amine upon solvation with acetonitrile (Figure 3). With acetonitrile as the guest, COF-300 adopts an expanded structure and COF-300-amine produces diffraction peaks that are also consistent with this structure, albeit with a larger *c*-axis (see page S3 for discussion). There is ambiguity to the exact

unit cell and space group of the acetonitrile-solvated COF-300-amine structure, but the pattern can be conservatively fit within the same space group as COF-300, $I4_1/a$. These results

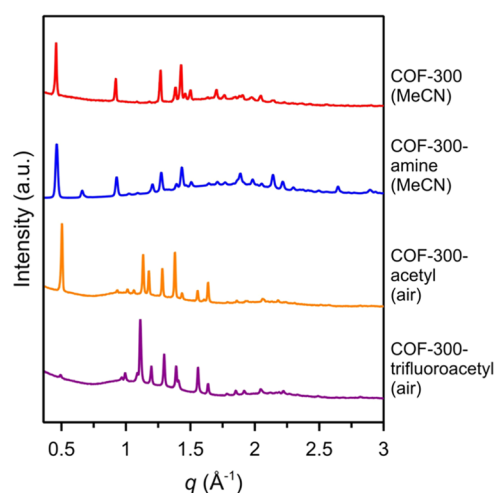


Figure 3. Powder X-ray diffraction (PXRD) data for the COF-300 derivatives. Red: COF-300 solvated in acetonitrile (MeCN). Blue: COF-300-amine solvated in acetonitrile (MeCN). Orange: COF-300-acetyl as-synthesized (air). Purple: COF-300-trifluoroacetyl as-synthesized (air).

suggest that the overall COF-300 framework is retained during reduction to COF-300-amine and that the materials derived from COF-300 have flexible structures. Furthermore, the PXRD patterns of the as-synthesized samples of COF-300-acetyl and COF-300-trifluoroacetyl (Figure 3) were revealed by Pawley fitting to belong to space group $I4_1/a$ (Figures S15–S16), consistent with the framework structure of COF-300.³²

In contrast, the PXRD patterns of COF-300-methyl and COF-300-dimethyl contain no sharp peaks (Figure S11). To determine whether the overall framework structure is maintained in the methylated and dimethylated materials, we imaged the particles by scanning electron microscopy (SEM). As seen in Figure 4, COF-300 appears as oblong particles, approximately 1 μm in length. Each of the postsynthetically modified materials retains the same morphology and particle size as COF-300, which indicates that the framework structure of COF-300-methyl and COF-300-dimethyl is retained upon methylation. Further, the continued presence of the benzylic

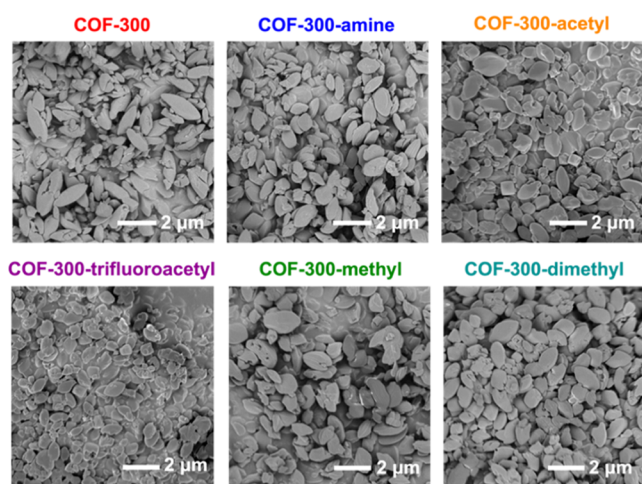


Figure 4. Scanning electron microscopy (SEM) images of COF-300 derivatives.

carbon in the ssNMR spectra of COF-300-methyl and COF-300-dimethyl belies any linkage degradation during the methylation reaction. We hypothesize that the lack of diffraction peaks by PXRD is due to the increased structural

disorder presented by the introduction of flexible, aliphatic amines.

The thermal stability of the materials was assessed by using thermogravimetric analysis (TGA). COF-300, COF-300-amine, COF-300-acetyl, and COF-300-trifluoroacetyl are stable until 400 °C. COF-300-methyl and COF-300-dimethyl, however, begin to decompose at 100 °C, with the decomposition rate being more rapid with increasing dimethylation (Figure S37). We hypothesize that a quaternary ammonium group bound to a benzylic position makes for a more labile C–N bond, thus reducing the material's thermal stability. While reduced thermal stability is a generally undesirable result in materials design, the 100 °C decomposition temperature for COF-300-methyl and COF-300-dimethyl has little bearing on their ability to adsorb PFAS from water sources (as it is most energy-efficient to perform this process at room temperature). In future work, we aim to improve the thermal stability of these materials by installing alkyl, rather than aryl, dimethylammonium groups, which will be less susceptible to nucleophilic attack at an adjacent carbon.

The permanent porosity of each of the materials was examined by obtaining N₂ isotherms at 77 K (Figures S21–S26). For COF-300, the Brunauer–Emmett–Teller (BET) surface area was determined to be 1359 m²/g, consistent with

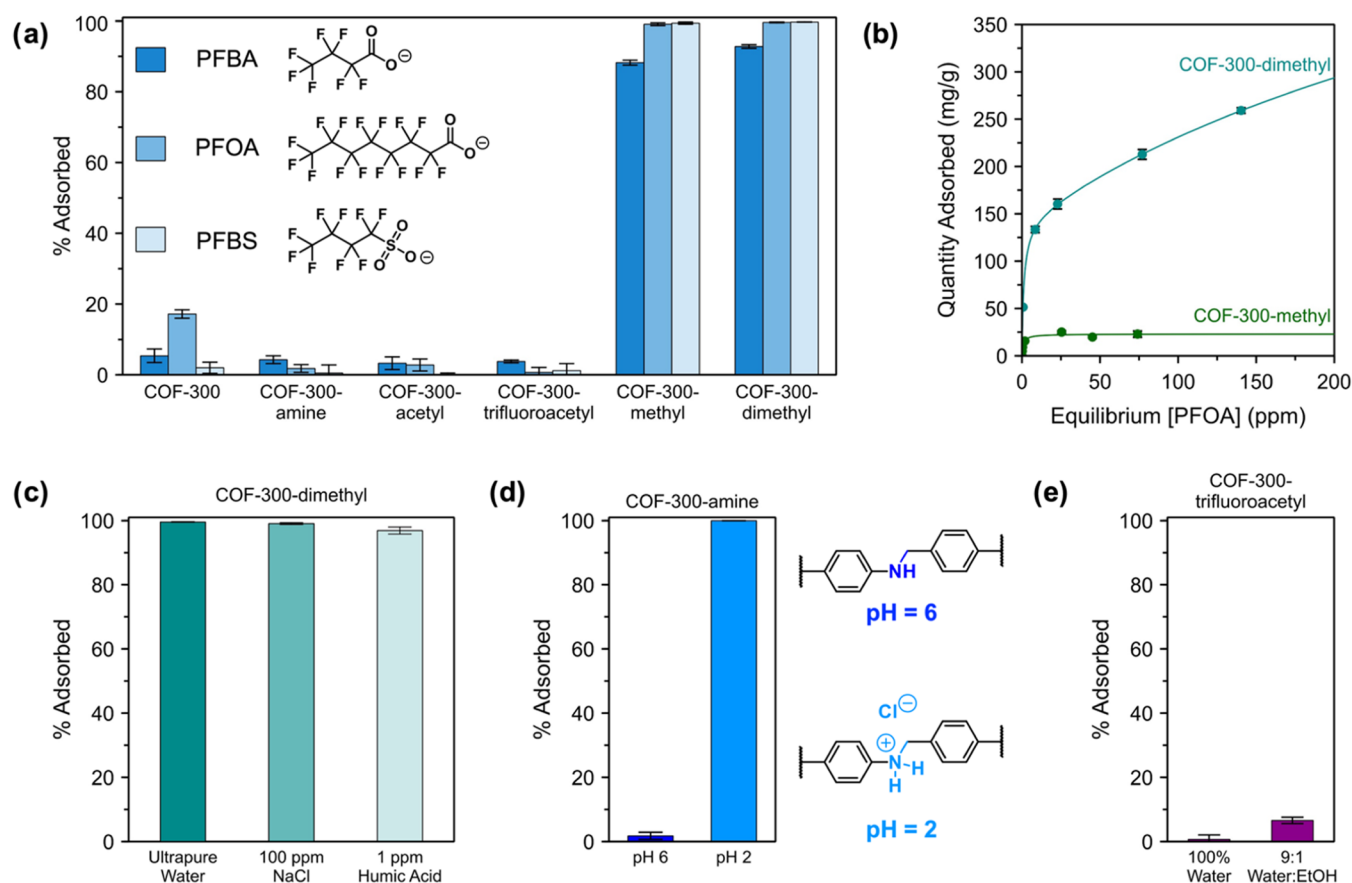


Figure 5. (a) Equilibrium removal percentage of PFAS molecules of varying chain length by equal mass concentrations of the different COFs after 18 h of contact time. [PFAS]₀ = 100 ppb, [COF] = 1 mg/1 g of PFAS solution. (b) PFOA adsorption isotherms for COF-300-methyl and COF-300-dimethyl after 18 h of contact time. [COF] = 1 mg/1 g PFOA solution. Circles represent adsorption data, and solid lines represent dual-site Langmuir fits. (c) PFOA adsorption by COF-300-dimethyl in ultrapure water, 100 ppm of NaCl, or 1 ppm of humic acid. [PFOA]₀ = 100 ppb, [COF] = 1 mg/1 g PFOA solution. (d) PFOA adsorption by COF-300-amine in pH 6 water and pH 2 water. pH 2 was achieved through the addition of HCl. (e) PFOA adsorption by COF-300-trifluoroacetyl in pure water and a 9:1 water:ethanol mixture. [PFOA]₀ = 100 ppb, [COF] = 1 mg/1 g PFAS solution. In all experiments, error bars are the standard deviation (1 sigma) of triplicate measurements.

its literature value.³⁰ However, each of the postsynthetically modified materials exhibited significantly lower surface areas (ranging from 2 to 13 m²/g). The reduction in surface area from COF-300 to COF-300-amine is supported by literature reports.³⁵ We hypothesize that increased framework flexibility resulting from imine reduction allows the COF-300 derivatives to contract under a vacuum, reducing their apparent porosity in BET measurements. However, PXRD experiments in which dry COF-300-amine undergoes a structural expansion when exposed to solvent (Figure S10), CO₂ adsorption measurements for COF-300-amine (Figure S45), and aqueous PFAS adsorption experiments (described below) indicate that these materials are significantly porous to solvent, CO₂, water, and dissolved PFAS molecules.

PFAS Adsorption Experiments. Each of the COF-300 derivatives was tested for its ability to adsorb sulfonate and carboxylate PFAS molecules of different chain lengths. The PFAS molecules selected were perfluorobutanoic acid (PFBA), perfluorooctanoic acid (PFOA), and perfluorobutanesulfonic acid (PFBS), as shown in Figure 5a. The PFAS adsorption capacity for each COF was assessed by submerging a dry COF sample in water containing 100 ppb of the different PFAS molecules; after an 18 h equilibration, the amount of PFAS remaining in solution was quantified by liquid chromatography–mass spectrometry (LC-MS). The difference between the starting PFAS concentration and equilibrium PFAS concentration was used to calculate the percent PFAS adsorbed by each COF (Figure 5a). The PFAS adsorption performance of COF-300 was unimpressive, and the reduced, acetylated, and trifluoroacetylated materials fared even worse. However, COF-300-methyl and COF-300-dimethyl showed dramatic increases in PFAS adsorption capacity, removing nearly 100% of PFOA and PFBS and more than 80% of PFBA.

Although COF-300-methyl and COF-300-dimethyl performed similarly well at PFAS concentrations in the parts per billion range, we wanted to test whether the degree of dimethylation affected the adsorption capacity at higher PFAS concentrations. To this end, PFOA adsorption isotherms were obtained for COF-300-methyl and COF-300-dimethyl, with equilibrium PFOA concentrations spanning the ppm range (Figure 5b). These experiments revealed that an increase in the degree of dimethylation leads to a major increase in the adsorption capacity: The PFOA adsorption capacity of COF-300-methyl plateaus at approximately 30 mg/g, but the capacity of COF-300-dimethyl adsorbs up to 259 mg/g at the concentrations tested. Because the moderate PFAS capacity of COF-300-methyl suggests the presence of some dimethylammonium sites in this material, we analyzed pristine samples of COF-300-methyl and COF-300-dimethyl through C/H/N combustion analysis and energy-dispersive X-ray (EDX) spectroscopy. The results of these analyses indicate that approximately 23–25% of the amine linkages in COF-300-methyl are dimethylated, while approximately 56–59% of the amine linkages in COF-300-dimethyl are dimethylated (see the Supporting Information for details). Thus, these dimethylammonium sites within COF-300-methyl are likely to be responsible for its modest PFAS adsorption shown in Figure 5b.

The PFOA adsorption capacity of COF-300-dimethyl is approximately 14,500 times greater than that of COF-300 (calculated from the capacity shown in Figure 5a), suggesting that the electrostatic interactions between the quaternary ammonium sites and the anionic PFAS molecules play a

significant role in the adsorption capacity. The high adsorption capacity of COF-300-dimethyl underscores the value of late-stage diversification in COF synthesis, as a simple linkage alkylation transforms the low-capacity framework COF-300 into an outstanding PFAS adsorbent.

Given the high PFOA adsorption capacity of COF-300-dimethyl, we performed multicomponent adsorption experiments to evaluate the influence of competing adsorbates on the PFAS capacity. Specifically, 100 ppb PFOA solutions were prepared in either 100 ppm of sodium chloride or 1 ppm of humic acid, and the ability of COF-300-dimethyl to adsorb PFOA in the presence of these species was tested. As shown in Figure 5c, COF-300-dimethyl was still able to adsorb nearly 100% of the PFOA in solution in the presence of a 100-fold excess of humic acid or a 1000-fold excess of NaCl.

Mechanism of Adsorption. The PFAS adsorption results described above indicate that the electrostatic interactions introduced by cationic ammonium sites have a major effect on the PFAS adsorption capacity. With this in mind, we were interested in whether the pH could affect the adsorption capacity of COF-300-amine. At a low pH, the secondary amines would be protonated, producing quaternary ammonium sites. We selected a pH of 2 as sufficiently low to protonate the secondary amines of COF-300-amine but not so low as to protonate the anionic PFAS molecules.^{36,37} Adsorption of PFOA by COF-300-amine was carried out at pH 2, as shown in Figure 5d. In comparison to PFOA adsorption at pH 6, the acidic adsorption experiments showed a significant enhancement in adsorption capacity, allowing the protonated COF-300-amine to adsorb 100% of the available PFOA. These results highlight the importance of electrostatic interactions in the high PFAS capacity of COF-300-dimethyl. On the other hand, COF-300-trifluoroacetyl displayed a surprisingly low PFAS adsorption capacity, despite being functionalized with a PFAS-targeting fluorocarbon group. We considered that the increased hydrophobicity of the fluorinated COF may have led to poor dispersion of the COF in water, thus inhibiting its ability to adsorb dissolved PFAS molecules. To test this, the PFOA adsorption experiments were repeated in a solution of 10% ethanol in water, to better disperse COF-300-trifluoroacetyl (Figure S32). As shown in Figure 5e, the addition of ethanol led to a minor enhancement in PFOA adsorption, but the overall capacity remained low. We hypothesize that hydrophobic interactions alone are not sufficient for a high PFAS capacity and that electrostatic interactions are a more important factor.

To test whether the COF-300-dimethyl could serve as a recyclable adsorbent, we attempted to desorb PFOA from the material after adsorption. Although we screened many regeneration conditions to desorb PFOA from COF-300-dimethyl, none were successful (page S6). In order to understand this inability to regenerate COF-300-dimethyl, we measured the thermodynamic parameters of PFOA binding using isothermal titration calorimetry (ITC; Figures 6 & S49).³⁸ The PFOA binding process was found to be endothermic, as indicated by a positive ΔH value of 2.14 ± 0.09 kcal/mol. This result is consistent with previous reports of endothermic PFAS binding in cationic polymers.³⁹ The positive and relatively large ΔS term ($T\Delta S = 9.61 \pm 0.10$ kcal/mol) leads to a negative ΔG value of -7.47 ± 0.05 kcal/mol, indicating that PFOA binding is thermodynamically favored. We hypothesize that the high entropic contribution may be due to the displacement of multiple adsorbed water

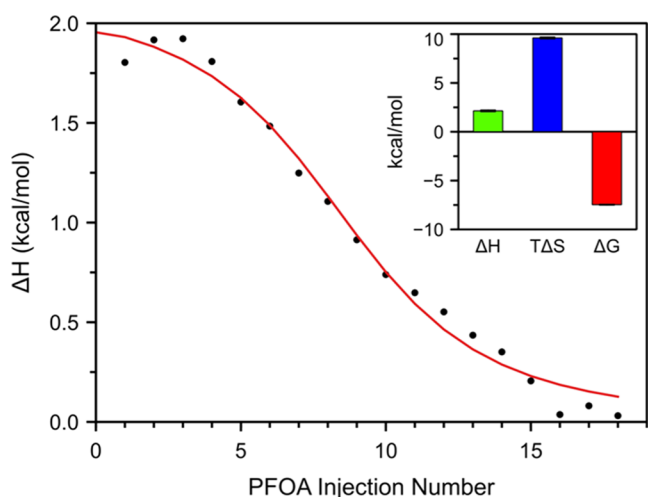


Figure 6. Plot of ΔH as a function of the PFOA injection number. The solid line represents the best nonlinear fit to a 1:1 binding model. Inset: Calculated thermodynamic parameters.

molecules per adsorbed PFOA molecule, which increases the overall disorder of the system. The ITC measurements yielded a PFOA binding constant of $(2.98 \pm 0.58) \times 10^5 \text{ M}^{-1}$ for COF-300-dimethyl, a relatively high value compared to PFAS binding in other COFs.⁸ The results of the ITC experiments, especially the large PFOA binding constant, suggest that strong, thermodynamically favored PFOA binding prevents facile regeneration of COF-300-dimethyl. To improve the recyclability of PFAS adsorbents, such as COF-300-dimethyl, future work will focus on balancing the thermodynamic trade-offs between strong PFAS binding and easy PFAS desorption. Pore engineering strategies that increase the hydrophilicity of the pore environment could offset the entropic gain from the release of adsorbed water molecules, resulting in less thermodynamically favored PFAS adsorption and easier subsequent PFAS desorption.

CONCLUSIONS

Although the three-dimensional framework COF-300 was first reported in 2009, until now chemists had not succeeded in functionalizing COF-300 beyond the addition of $-\text{OH}$ or $-\text{Br}$ groups.^{40–43} Herein, we have shown that linkage transformation is a versatile way to functionalize COF-300 with alkyl, acetyl, or trifluoroacetyl groups. The resulting library of COF-300 derivatives led to the discovery of an outstanding PFAS adsorbent, COF-300-dimethyl, with a saturation capacity for perfluorooctanoic acid exceeding 250 mg/g. Further, by readily generating and testing a range of functionalized materials, the linker-functionalization approach allowed us to quickly establish design principles for future PFAS adsorbents. The significance of this approach extends beyond COF-300 to a broader class of imine-linked COFs: Linkage functionalization eliminates the need to install functional groups onto COF building blocks and thus offers a shortened route to functionalized three-dimensional frameworks.

ASSOCIATED CONTENT

Supporting Information

The Supporting Information is available free of charge at <https://pubs.acs.org/doi/10.1021/acsami.3c12826>.

General procedures, synthetic procedures, and supplementary figures (PDF)

AUTHOR INFORMATION

Corresponding Author

Mercedes K. Taylor – Department of Chemistry and Biochemistry, University of Maryland, College Park, Maryland 20742, United States; orcid.org/0000-0002-0945-766X; Email: mkt@umd.edu

Authors

Andrea N. Zeppuhar – Department of Chemistry and Biochemistry, University of Maryland, College Park, Maryland 20742, United States; orcid.org/0000-0003-1863-7360

Devin S. Rollins – Department of Chemistry, University of Washington, Seattle, Washington 98195, United States

Dale L. Huber – Center for Integrated Nanotechnologies, Sandia National Laboratories, Albuquerque, New Mexico 87123, United States; orcid.org/0000-0001-6872-8469

Emmanuel A. Bazan-Bergamino – Department of Chemistry and Biochemistry, University of Maryland, College Park, Maryland 20742, United States

Fu Chen – Department of Chemistry and Biochemistry, University of Maryland, College Park, Maryland 20742, United States

Hayden A. Evans – Center for Neutron Research, National Institute of Standards and Technology, Gaithersburg, Maryland 20878, United States; orcid.org/0000-0002-1331-4274

Complete contact information is available at: <https://pubs.acs.org/doi/10.1021/acsami.3c12826>

Notes

The authors declare no competing financial interest.

ACKNOWLEDGMENTS

The authors thank the University of Maryland, College Park, for funding. They acknowledge Dr. Yue Li and the Mass Spectrometry Facility in the Department of Chemistry and Biochemistry at the University of Maryland, College Park, for use of the Bruker Maxis-II QTOF mass spectrometer. Purchase of the Bruker Maxis-II QTOF mass spectrometer was supported by NSF Award Number 2018860. The authors thank the National Science Foundation (NSF-1726058) for funding a solid-state NMR spectrometer. They acknowledge the support of the Maryland NanoCenter and its AIMLab. They gratefully acknowledge the support of the Center for Integrated Nanotechnologies, an Office of Science User Facility operated for the US DOE Office of Science. Sandia National Laboratories is a multimission laboratory managed and operated by National Technology and Engineering Solutions of Sandia, LLC, a wholly owned subsidiary of Honeywell International, Inc., for the US DOE's National Nuclear Security Administration (contract no. DE-NA-0003525). The views expressed in the article do not necessarily represent the views of the US DOE or the US government. Powder X-ray diffraction data were collected on beamline 17-BM at the Advanced Photon Source at Argonne National Laboratory, which is supported by the U.S. Department of Energy, Office of Science, Office of Basic Energy Sciences under Contract DEAC02-06CH11357. Certain commercial

equipment, instruments, or materials are identified in this document. Such identification does not imply recommendation or endorsement by the National Institute of Standards and Technology, nor does it imply that the products identified are necessarily the best available for the purpose.

REFERENCES

- (1) Jiang, Y.; Liu, C.; Huang, A. EDTA-Functionalized Covalent Organic Framework for the Removal of Heavy-Metal Ions. *ACS Appl. Mater. Interfaces* **2019**, *11* (35), 32186–32191.
- (2) Li, Y.; Wang, C.; Ma, S.; Zhang, H.; Ou, J.; Wei, Y.; Ye, M. Fabrication of Hydrazone-Linked Covalent Organic Frameworks Using Alkyl Amine as Building Block for High Adsorption Capacity of Metal Ions. *ACS Appl. Mater. Interfaces* **2019**, *11* (12), 11706–11714.
- (3) Li, L.; Zhou, Z.; Li, L.; Zhuang, Z.; Bi, J.; Chen, J.; Yu, Y.; Yu, J. Thioether-Functionalized 2D Covalent Organic Framework Featuring Specific Affinity to Au for Photocatalytic Hydrogen Production from Seawater. *ACS Sustainable Chem. Eng.* **2019**, *7* (22), 18574–18581.
- (4) Pan, X.; Qin, X.; Zhang, Q.; Ge, Y.; Ke, H.; Cheng, G. N- and S-rich covalent organic framework for highly efficient removal of indigo carmine and reversible iodine capture. *Microporous Mesoporous Mater.* **2020**, *296*, No. 109990.
- (5) Yu, S.-B.; Lyu, H.; Tian, J.; Wang, H.; Zhang, D.-W.; Liu, Y.; Li, Z.-T. A polycationic covalent organic framework: a robust adsorbent for anionic dye pollutants. *Polym. Chem.* **2016**, *7* (20), 3392–3397.
- (6) Ji, W.; Xiao, L.; Ling, Y.; Ching, C.; Matsumoto, M.; Bisbey, R. P.; Helbling, D. E.; Dichtel, W. R. Removal of GenX and Perfluorinated Alkyl Substances from Water by Amine-Functionalized Covalent Organic Frameworks. *J. Am. Chem. Soc.* **2018**, *140* (40), 12677–12681.
- (7) Hou, Y.-J.; Deng, J.; He, K.; Chen, C.; Yang, Y. Covalent Organic Frameworks-Based Solid-Phase Microextraction Probe for Rapid and Ultrasensitive Analysis of Trace Per- and Polyfluoroalkyl Substances Using Mass Spectrometry. *Anal. Chem.* **2020**, *92* (15), 10213–10217.
- (8) Huang, J.; Shi, Y.; Huang, G.-z.; Huang, S.; Zheng, J.; Xu, J.; Zhu, F.; Ouyang, G. Facile Synthesis of a Fluorinated-Squaramide Covalent Organic Framework for the Highly Efficient and Broad-Spectrum Removal of Per- and Polyfluoroalkyl Pollutants. *Angew. Chem., Int. Ed.* **2022**, *61* (31), No. e202206749, DOI: 10.1002/anie.202206749.
- (9) Liu, H.; Chu, J.; Yin, Z.; Cai, X.; Zhuang, L.; Deng, H. Covalent Organic Frameworks Linked by Amine Bonding for Concerted Electrochemical Reduction of CO₂. *Chem* **2018**, *4* (7), 1696–1709.
- (10) Yan, Q.; Xu, H.; Jing, X.; Hu, H.; Wang, S.; Zeng, C.; Gao, Y. Post-synthetic modification of imine linkages of a covalent organic framework for its catalysis application. *RSC Adv.* **2020**, *10* (30), 17396–17403.
- (11) Waller, P. J.; Lyle, S. J.; Osborn Popp, T. M.; Diercks, C. S.; Reimer, J. A.; Yaghi, O. M. Chemical Conversion of Linkages in Covalent Organic Frameworks. *J. Am. Chem. Soc.* **2016**, *138* (48), 15519–15522.
- (12) Waller, P. J.; AlFaraj, Y. S.; Diercks, C. S.; Jarenwattananon, N. N.; Yaghi, O. M. Conversion of Imine to Oxazole and Thiazole Linkages in Covalent Organic Frameworks. *J. Am. Chem. Soc.* **2018**, *140* (29), 9099–9103.
- (13) Li, X.; Zhang, C.; Cai, S.; Lei, X.; Altoe, V.; Hong, F.; Urban, J. J.; Ciston, J.; Chan, E. M.; Liu, Y. Facile transformation of imine covalent organic frameworks into ultrastable crystalline porous aromatic frameworks. *Nat. Commun.* **2018**, *9* (1), No. 2998, DOI: 10.1038/s41467-018-05462-4.
- (14) Sun, Q.; Aguila, B.; Perman, J.; Earl, L. D.; Abney, C. W.; Cheng, Y.; Wei, H.; Nguyen, N.; Wojtas, L.; Ma, S. Postsynthetically Modified Covalent Organic Frameworks for Efficient and Effective Mercury Removal. *J. Am. Chem. Soc.* **2017**, *139* (7), 2786–2793.
- (15) Khojastehnezhad, A.; Moeinpour, F.; Jafari, M.; Shehab, M. K.; ElDouhaibi, A. A. S.; El-Kaderi, H. M.; Sijaj, M. Postsynthetic Modification of Core–Shell Magnetic Covalent Organic Frameworks for the Selective Removal of Mercury. *ACS Appl. Mater. Interfaces* **2023**, *15* (23), 28476–28490, DOI: 10.1021/acsami.3c02914.
- (16) Grunenberg, L.; Savasci, G.; Emmerling, S. T.; Heck, F.; Bette, S.; Cima Bergesch, A.; Ochsenfeld, C.; Lotsch, B. V. Postsynthetic Transformation of Imine- into Nitron-Linked Covalent Organic Frameworks for Atmospheric Water Harvesting at Decreased Humidity. *J. Am. Chem. Soc.* **2023**, *145* (24), 13241–13248.
- (17) Mitra, S.; Sasmal, H. S.; Kundu, T.; Kandambeth, S.; Illath, K.; Díaz Díaz, D.; Banerjee, R. Targeted Drug Delivery in Covalent Organic Nanosheets (CONs) via Sequential Postsynthetic Modification. *J. Am. Chem. Soc.* **2017**, *139* (12), 4513–4520.
- (18) Kurwadkar, S.; Dane, J.; Kanel, S. R.; Nadagouda, M. N.; Cawdrey, R. W.; Ambade, B.; Struckhoff, G. C.; Wilkin, R. Per- and polyfluoroalkyl substances in water and wastewater: A critical review of their global occurrence and distribution. *Sci. Total Environ.* **2022**, *809*, No. 151003.
- (19) Johnson, G. R.; Brusseau, M. L.; Carroll, K. C.; Tick, G. R.; Duncan, C. M. Global distributions, source-type dependencies, and concentration ranges of per- and polyfluoroalkyl substances in groundwater. *Sci. Total Environ.* **2022**, *841*, No. 156602.
- (20) Evich, M. G.; Davis, M. J. B.; McCord, J. P.; Acrey, B.; Awkerman, J. A.; Knappe, D. R. U.; Lindstrom, A. B.; Speth, T. F.; Tebes-Stevens, C.; Strynar, M. J.; Wang, Z.; Weber, E. J.; Henderson, W. M.; Washington, J. W. Per- and polyfluoroalkyl substances in the environment. *Science*, *375* 6580 eabg9065 DOI: 10.1126/science.abg9065.
- (21) Brunn, H.; Arnold, G.; Körner, W.; Rippen, G.; Steinhäuser, K. G.; Valentin, I. PFAS: forever chemicals—persistent, bioaccumulative and mobile. Reviewing the status and the need for their phase out and remediation of contaminated sites. *Environ. Sci. Eur.* **2023**, *35* (1), No. 20, DOI: 10.1186/s12302-023-00721-8.
- (22) Fenton, S. E.; Ducatman, A.; Boobis, A.; DeWitt, J. C.; Lau, C.; Ng, C.; Smith, J. S.; Roberts, S. M. Per- and Polyfluoroalkyl Substance Toxicity and Human Health Review: Current State of Knowledge and Strategies for Informing Future Research. *Environ. Toxicol. Chem.* **2021**, *40* (3), 606–630.
- (23) Panieri, E.; Baralic, K.; Djukic-Cosic, D.; Buha Djordjevic, A.; Saso, L. PFAS Molecules: A Major Concern for the Human Health and the Environment. *Toxics* **2022**, *10*, No. 44, DOI: 10.3390/toxics10020044.
- (24) Kumarasamy, E.; Manning, I. M.; Collins, L. B.; Coronell, O.; Leibfarth, F. A. Ionic Fluorogels for Remediation of Per- and Polyfluorinated Alkyl Substances from Water. *ACS Cent. Sci.* **2020**, *6* (4), 487–492.
- (25) Manning, I. M.; Guan Pin Chew, N.; Macdonald, H. P.; Miller, K. E.; Strynar, M. J.; Coronell, O.; Leibfarth, F. A. Hydrolytically Stable Ionic Fluorogels for High-Performance Remediation of Per- and Polyfluoroalkyl Substances (PFAS) from Natural Water. *Angew. Chem., Int. Ed.* **2022**, *61* (41), No. e202208150, DOI: 10.1002/anie.202208150.
- (26) Wang, W.; Zhou, Z.; Shao, H.; Zhou, S.; Yu, G.; Deng, S. Cationic covalent organic framework for efficient removal of PFOA substitutes from aqueous solution. *Chem. Eng. J.* **2021**, *412*, No. 127509.
- (27) Tang, S.; Qin, X.; Lv, Y.; Hu, K.; Zhao, S. Adsorption of three perfluoroalkyl sulfonate compounds from environmental water and human serum samples using cationic porous covalent organic framework as adsorbents and detection combination with MALDI-TOF MS. *Appl. Surf. Sci.* **2022**, *601*, No. 154224.
- (28) Jia, Y.; Qian, J.; Pan, B. Dual-Functionalized MIL-101(Cr) for the Selective Enrichment and Ultrasensitive Analysis of Trace Per- and Poly-fluoroalkyl Substances. *Anal. Chem.* **2021**, *93* (32), 11116–11122.
- (29) Song, C.; Zheng, J.; Zhang, Q.; Yuan, H.; Yu, A.; Zhang, W.; Zhang, S.; Ouyang, G. Multifunctionalized Covalent Organic Frameworks for Broad-Spectrum Extraction and Ultrasensitive Analysis of Per- and Polyfluoroalkyl Substances. *Anal. Chem.* **2023**, *95* (19), 7770–7778.

- (30) Uribe-Romo, F. J.; Hunt, J. R.; Furukawa, H.; Klöck, C.; O’Keeffe, M.; Yaghi, O. M. A Crystalline Imine-Linked 3-D Porous Covalent Organic Framework. *J. Am. Chem. Soc.* **2009**, *131* (13), 4570–4571.
- (31) Ma, T.; Li, J.; Niu, J.; Zhang, L.; Etman, A. S.; Lin, C.; Shi, D.; Chen, P.; Li, L.-H.; Du, X.; Sun, J.; Wang, W. Observation of Interpenetration Isomerism in Covalent Organic Frameworks. *J. Am. Chem. Soc.* **2018**, *140* (22), 6763–6766.
- (32) Ma, T.; Kapustin, E. A.; Yin, S. X.; Liang, L.; Zhou, Z.; Niu, J.; Li, L.-H.; Wang, Y.; Su, J.; Li, J.; Wang, X.; Wang, W. D.; Wang, W.; Sun, J.; Yaghi, O. M. Single-crystal x-ray diffraction structures of covalent organic frameworks. *Science* **2018**, *361* (6397), 48–52.
- (33) Fischbach, D. M.; Rhoades, G.; Espy, C.; Goldberg, F.; Smith, B. J. Controlling the crystalline structure of imine-linked 3D covalent organic frameworks. *Chem. Commun.* **2019**, *55* (25), 3594–3597.
- (34) Chen, Y.; Shi, Z.-L.; Wei, L.; Zhou, B.; Tan, J.; Zhou, H.-L.; Zhang, Y.-B. Guest-Dependent Dynamics in a 3D Covalent Organic Framework. *J. Am. Chem. Soc.* **2019**, *141* (7), 3298–3303.
- (35) Jin, P.; Niu, X.; Zhang, F.; Dong, K.; Dai, H.; Zhang, H.; Wang, W.; Chen, H.; Chen, X. Stable and Reusable Light-Responsive Reduced Covalent Organic Framework (COF-300-AR) as a Oxidase-Mimicking Catalyst for GSH Detection in Cell Lysate. *ACS Appl. Mater. Interfaces* **2020**, *12* (18), 20414–20422.
- (36) Ulgen, M.; Gorrod, J. W.; Barlow, D. Structure-activity relationships in the formation of amides from substituted N-benzylanilines. *Xenobiotica* **1994**, *24* (8), 735–748.
- (37) Rayne, S.; Forest, K. Theoretical studies on the pKa values of perfluoroalkyl carboxylic acids. *J. Mol. Struct.: THEOCHEM* **2010**, *949* (1), 60–69.
- (38) Sha, F.; Tai, T.-Y.; Gaidimas, M. A.; Son, F. A.; Farha, O. K. Leveraging Isothermal Titration Calorimetry to Obtain Thermodynamic Insights into the Binding Behavior and Formation of Metal–Organic Frameworks. *Langmuir* **2022**, *38* (22), 6771–6779.
- (39) Tan, X.; Sawczyk, M.; Chang, Y.; Wang, Y.; Usman, A.; Fu, C.; Král, P.; Peng, H.; Zhang, C.; Whittaker, A. K. Revealing the Molecular-Level Interactions between Cationic Fluorinated Polymer Sorbents and the Major PFAS Pollutant PFOA. *Macromolecules* **2022**, *55* (3), 1077–1087.
- (40) Li, Z.; Ding, X.; Feng, Y.; Feng, W.; Han, B.-H. Structural and Dimensional Transformations between Covalent Organic Frameworks via Linker Exchange. *Macromolecules* **2019**, *52* (3), 1257–1265.
- (41) Mow, R. E.; Metzroth, L. J. T.; Dzara, M. J.; Russell-Parks, G. A.; Johnson, J. C.; Vardon, D. R.; Pylypenko, S.; Vyas, S.; Gennett, T.; Braunecker, W. A. Phototriggered Desorption of Hydrogen, Ethylene, and Carbon Monoxide from a Cu(I)-Modified Covalent Organic Framework. *J. Phys. Chem. C* **2022**, *126* (35), 14801–14812.
- (42) Mohammed, A. K.; Al Khoori, A. A.; Addicoat, M. A.; Varghese, S.; Othman, I.; Jaoude, M. A.; Polychronopoulou, K.; Baias, M.; Haija, M. A.; Shetty, D. Solvent-Influenced Fragmentations in Free-Standing Three-Dimensional Covalent Organic Framework Membranes for Hydrophobicity Switching. *Angew. Chem., Int. Ed.* **2022**, *61* (13), No. e202200905, DOI: 10.1002/anie.202200905.
- (43) Mohammed, A. K.; Ali, J. K.; Kuzhimully, M. B. S.; Addicoat, M. A.; Varghese, S.; Baias, M.; Alhseinat, E.; Shetty, D. The fragmented 3D-covalent organic framework in cellulose acetate membrane for efficient phenol removal. *Chem. Eng. J.* **2023**, *466*, No. 143234.